Published in Solar Energy Materials and Solar Cells 91, issue 6, 495-502, 2007
which should be used for any reference to this work

Microcrystalline silicon deposited at high rate on large areas from pure silane with efficient gas utilization

B. Strahm[a,*], A.A. Howling[a], L. Sansonnens[a], Ch. Hollenstein[a], U. Kroll[b], J. Meier[b], Ch. Ellert[b], L. Feitknecht[c], C. Ballif[c]

[a]*Ecole Polytechnique Fédérale de Lausanne (EPFL), Centre de Recherches en Physique des Plasmas, CH-1015 Lausanne, Switzerland*
[b]*Oerlikon Solar-Lab, Rue du Puits-Godet 12a, CH-2000 Neuchâtel, Switzerland*
[c]*Institut de Microtechnique, Université de Neuchâtel, Rue A.-L. Breguet 2, CH-2000 Neuchâtel, Switzerland*

Abstract

Microcrystalline silicon thin film deposited by RF-PECVD and integrated in a tandem structure is a promising material for low cost photovoltaic solar cells compared to solar cells based on crystalline silicon. However, in order to allow a cost-effective mass production of solar cells based on this material, deposition processes should fulfill several conditions such as high deposition rate, good uniformity over large area and efficient gas utilization. In this work, it is shown that the atomic hydrogen density can be high enough to form microcrystalline thin films even from a pure silane RF discharge and that the pure silane regime is more efficient in terms of gas utilization. In situ Fourier transform infrared absorption and ex situ Raman spectroscopy measurements have been used to determine the fraction of dissociated silane in the discharge and the crystallinity of the deposited layers. Results have shown that microcrystalline silicon can be deposited uniformly on a large area substrate with a deposition rate of more than 10 Å/s with a low powder formation and an input power density of 0.28 W cm^{-2} from a pure silane discharge.

Keywords: μc-Si:H; RF PECVD; Pure silane; High deposition rate; Large area

1. Introduction

Microcrystalline hydrogenated silicon (μc-Si:H) semiconductor devices such as photovoltaic (PV) solar cells properly prepared do not show the light-induced degradation compared to those based on amorphous hydrogenated silicon (a-Si:H) [1]. Moreover, the lower band gap of μc-Si:H compared to the one of a-Si:H gives a promising future to tandem PV cells [2]. However, the indirect bandgap of μc-Si:H means that thick μc-Si:H layers have to be deposited compared to thin a-Si:H films [1]. A good deposition process for PV solar cell production has to fulfill several conditions to assure cost-effective production: in order to reduce the processing time, the μc-Si:H deposition rate should ideally be higher than 10 Å/s. A uniformity better than ±10% over large area glass substrates (typically 1 m^2) has to be achieved in terms of thickness and material crystallinity. Moreover, powder formation in the discharge has to be avoided, because of the down time due to system (reactor, pumps, etc.) maintenance, non-uniformity of the deposited film due to powder clouds and furthermore, the potential health problem associated with fine particles. Polysilane formation also reduces the silane gas utilization efficiency by consuming the raw material (silicon atoms) needed for the film growth and, hence, it is difficult to reach high deposition rates in dusty conditions or with a high rate of polysilanes formation. In order to reduce problems associated with powder formation [3], film damage by high energy ion bombardment [4], arcing and parasitic plasmas [5], it would be desirable to apply a low RF input power. With regard to these observations, the ultimate cost-effective μc-Si:H deposition process should fulfill five conditions: the deposited film should be *uniform over large*

* Corresponding author.
E-mail address: benjamin.strahm@epfl.ch (B. Strahm).

areas, deposited at *high rate* with a *high gas utilization efficiency* from a *powder-free* plasma with *low power density*.

Deposition of μc-Si:H on large area substrates is generally performed by chemical vapor deposition (CVD) techniques such as hot-wire CVD and plasma-enhanced CVD (PECVD) from low silane (SiH_4) concentration ($<10\%$) mixtures in a hydrogen (H_2) background. This strong hydrogen dilution technique has been introduced because of the primary role of atomic hydrogen in the growth of microcrystalline silicon. The flux of hydrogen atoms to the growing surface has to be large compared to the silane radical flux in order to grow crystalline material. In the hydrogen dilution technique, the large atomic hydrogen flux to the surface compared to the silane radical flux is guaranteed by the large initial pressure of H_2 compared to the SiH_4 partial pressure. However, nothing prevents μc-Si:H deposition from pure silane plasma, because the deposition conditions depend on the plasma composition [6], which is very different from the input silane concentration in highly depleted plasmas, as shown by crystalline material deposited by high power density PECVD in small size reactors [7–10] from pure silane. Previous work [11] has shown that with a large initial silane concentration and a high depletion of silane in the plasma, the silane partial pressure in the plasma becomes as low as in strongly hydrogen-diluted plasmas. Hence, a similar ratio of atomic hydrogen to silane radical fluxes to the surface can be reached even with a large ($>10\%$) initial silane concentration.

In spite of the promising gas utilization efficiency of pure silane processes [8], up to now μc-Si:H deposition over large areas has been investigated only for the conventional hydrogen-diluted regime [12,13], and a pure silane process has never been tested in systems larger than small laboratory reactors. Even in these small reactors, the highest deposition rate recorded is less than $10\,\text{Å/s}$ although higher deposition rates of solar grade material have been demonstrated in the case of the hydrogen-diluted regime [14–16].

The aim of this work is to show the feasibility of the deposition of μc-Si:H from pure silane plasma on large area substrates with a high gas utilization efficiency, hence coming closer to the ultimate cost-effective process for PV mass production. In this work, a large area industrial plasma reactor with an in situ Fourier transform infrared (FTIR) absorption diagnostic was used to measure the plasma composition which is a determining factor for the deposited material microstructure (Section 3.1). Sections 3.2 and 3.3 will present the results of the films crystallinity and plasma composition as a function of the initial silane concentration. In particular it will be shown that high deposition rates with high efficiency of gas utilization without wasting a large fraction of silane gas to the pumps or as powder can be attained even with high input silane concentration. Finally, a simple method to estimate the polysilane or powder fraction lost in the pumping line will be presented in Section 3.4.

2. Experimental setup and methods

The experimental arrangement presented in Fig. 1 consists of a radio-frequency (RF) capacitively coupled plasma-enhanced chemical vapor deposition (PECVD) reactor equipped with an in situ FTIR absorption spectrometer. The plasma reactor is a modified version of an industrial KAI-S reactor based on the PlasmaBox® concept [17] developed by UNAXIS Ltd. for large area substrates ($37 \times 47\,\text{cm}^2$). It consists of a grounded $47 \times 57\,\text{cm}^2$ aluminum box placed in a large vacuum chamber. The RF powered electrode is suspended inside the grounded box at a distance of 25 mm from the grounded base (Fig. 1(b)). Process gases (silane and hydrogen) are introduced into the reactor through the RF electrode via a uniform showerhead and are pumped out from one side through a pumping grid in order to provide a uniform distribution of all gases over the whole substrate area [18].

Experiments were performed where the silane concentration was varied from 2.7% to 100% corresponding to a hydrogen flow rate from 3000 to 0 sccm. Depositions were

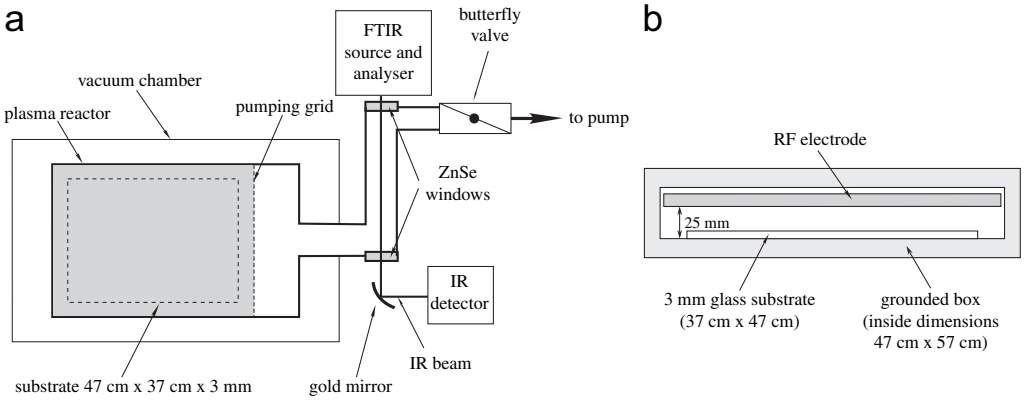

Fig. 1. (a) Top view of the $47 \times 57\,\text{cm}^2$ PECVD reactor, vacuum chamber and FTIR equipment used to measure the silane density in the exhaust line; (b) lateral view of the deposition reactor with the RF electrode suspended in the grounded aluminum box.

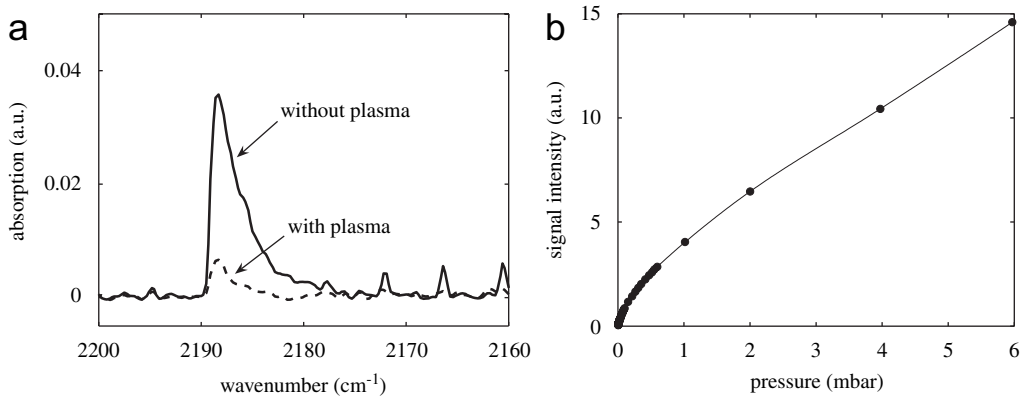

Fig. 2. (a) IR absorption spectra of silane without (solid line) and with (dashed line) discharge for a 2% SiH_4-H_2 mixture at 4 mbar (taken from Ref. [11]) and (b) calibration curve measured from pure silane gas as a function of pressure used to determine silane partial pressure with and without plasma in the reactor.

performed on 3 mm thick glass substrates ($37 \times 47\,cm^2$) at an excitation frequency of 40.68 MHz, a substrate temperature of 230 °C, and within a pressure range from 0.5 to 10 mbar. The RF power input was varied from 150 to 2000 W. The reactor was cleaned before each deposition with a chemical etching plasma, using SF_6, to guarantee reproducibility.

In situ FTIR absorption spectroscopy (Bruker Equinox 55 with an external detector Graseby type FTIR-W24) was performed by a single pass (path length of 1 m) measurement in the exhaust line of the reactor through two ZnSe windows, as shown in Fig. 1(a). This arrangement was used to determine the partial pressure of silane in the exhaust flow with, p_{SiH_4}, and without, $p^0_{SiH_4}$, discharge in the reactor. These pressures were measured by integrating the IR absorption spectra (Fig. 2(a)) from 2199 to 2163 cm^{-1} (SiH_4 Q branch) and by using a calibration curve performed with pure silane gas (without any H_2 dilution) for pressures from 0.05 to 6 mbar (see Fig. 2(b)). The silane concentration *in the plasma* is defined as

$$c_p = \frac{p_{SiH_4}}{p}, \tag{1}$$

and the silane initial concentration c is defined as

$$c = \frac{p^0_{SiH_4}}{p}, \tag{2}$$

where $p^0_{SiH_4}$ is the silane partial pressure without plasma and p is the total pressure which is maintained constant during the measurement. This definition of the initial silane concentration in terms of pressures instead of flow rates avoids errors due to possible different pumping speeds of silane and hydrogen. The silane concentration in the plasma, c_p, can be related to the silane depletion fraction D and the input silane concentration c for uniform showerhead reactor with uniform plasma only [11,18]

$$c_p = (1 - D)c, \tag{3}$$

where the silane depletion fraction D in the discharge is defined as

$$D = \frac{p^0_{SiH_4} - p_{SiH_4}}{p^0_{SiH_4}}. \tag{4}$$

Further details on FTIR measurements of silane in plasma are described by Sansonnens et al. [19].

Deposition rates were measured in situ by monochromatic light interferometry at the center of the substrate and the deposition time was adjusted in order to have a film thickness of approximately 200 nm. This thickness guarantees that the final microstructure is reached since, in our system, the plasma chemical equilibrium is attained in less than 1 s after plasma ignition, as observed by optical emission spectroscopy. This means that the microstructure evolution due to plasma variation during deposition is confined to the first atomic layers of the film, even for high deposition rates. Thickness uniformity measurements were performed on the 3 mm thick glass substrate. The uniformity was measured on the whole substrate area by white light interferometry. Micro-Raman spectroscopy (Renishaw RM series Raman microscope) was used to determine the crystallinity factor ϕ_c of the deposited material as the ratio of the area of the Raman peaks associated with crystalline materials centered at 510 and 518 cm^{-1} to the total peak area including the amorphous peak centered at 480 cm^{-1} [20].

3. Results and discussion

3.1. Microstructure and plasma composition

The Raman crystallinity of films deposited under various conditions (total gas flow rate from 0.5 to 4 slm, pressure from 0.5 to 10 mbar, silane initial concentration from 0.5% to 10% and RF power input from 500 to 2000 W) is plotted against the initial silane concentration, c, in Fig. 3(a). These results show that the input silane concentration alone is not a relevant factor for the determination of the deposited material microstructure if the other deposition

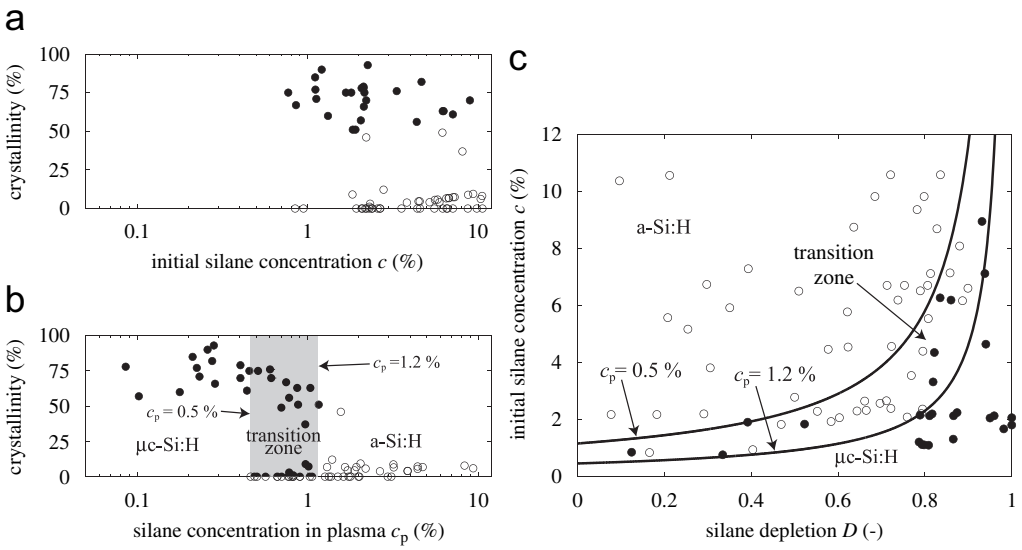

Fig. 3. Plot of Raman crystallinity as a function of (a) the input silane concentration c and (b) the silane concentration in the plasma c_p and (c) two-dimensional representation of the three microstructure regions as a function of depleted silane fraction D and input silane concentration c. Data are sorted as a function of their crystallinity: µc-Si:H (•) for $\phi_c > 50\%$ and a-Si:H (○) for $\phi_c < 50\%$. The transition zone is only valid for the substrate temperature used for experimental results ($T_s = 230\,^{\circ}\mathrm{C}$). Taken from Ref. [11].

parameters are not fixed as has been done in many works [21–25]. On the other hand, if the crystallinity of the same samples is plotted as a function of the silane concentration *in the plasma*, c_p, as in Fig. 3(b), samples are arranged into three distinct regions. A microcrystalline region ($c_p < 0.5\%$) is separated from an amorphous region ($c_p > 1.2\%$) by a transition zone where the material crystallinity is not well defined and can have values from 0 to 75%. The fact that the silane concentration in the plasma depends on the input silane concentration c and on the silane depletion fraction D through Eq. (3) allows a two-dimensional representation of the three regions as presented in Fig. 3(c).

3.2. Effect of H_2 dilution on the deposition rate and silane gas utilization fraction

Experimental data presented in Fig. 3 show that c_p is a relevant parameter for the determination of the microstructure transition, but the range in silane concentration (0–10%) was limited to concentrations conventionally used to deposit µc-Si:H films. However, Eq. (3) predicts µc-Si:H deposition even from a pure silane plasma ($c = 1$), if the silane depletion D is sufficiently high ($D > 0.995$) to maintain $c_p < 0.5\%$. Physically, this is because a highly depleted silane plasma consists mostly of hydrogen [6,11] and, therefore, the plasma chemistry behaves similarly to a low depletion plasma with a strong hydrogen dilution. To reach such high silane depletion, the dissociation rate and the gas residence time have to be as high as possible. Moreover, with a high depletion plasma, it is only necessary to feed into the reactor the required silane flow to reach a target deposition rate, because all the silane molecules are dissociated and deposited. Hence, we can estimate the deposition rate for a given silane flow rate: assuming that every silicon atom flowing into the reactor is deposited uniformly on the reactor surface (no silane, SiH_x radicals nor polysilanes is pumped out) and that the deposited layer has a density ρ of $2180\,\mathrm{kg\,m^{-3}}$ [26], then the maximum possible deposition rate (R_{max}) is given by

$$R_{max} = \frac{\Phi_{SiH_4} V m_{Si}}{A\rho}(\mathrm{m/s}) = 0.0962\frac{F_{SiH_4}}{A}(\mathrm{A/s}), \qquad (5)$$

where A is the total area of the reactor surface facing the plasma in m^2 and V the reactor volume in m^3, Φ_{SiH_4} and F_{SiH_4} the silane flow rate in $\mathrm{mol\,m^{-3}\,s^{-1}}$ and sccm, respectively, and m_{Si} the mass of the silicon atom in kg. Thus, if we fix the target deposition rate at $10\,\mathrm{\AA/s}$ and assume a maximum loss fraction of 25% of the input silane flow rate, the required input silane flow rate is 82 sccm for the KAI-S deposition reactor with an electrode area of $0.593\,m^2$. For all the following results, the silane flow rate is fixed at 82 sccm ($R_{max} = 13.3\,\mathrm{\AA/s}$) and therefore, the only way to reach the pure silane regime from the standard H_2 diluted one is by decreasing the H_2 flow and, hence, increasing the silane input concentration.

Results performed with an input power of 1000 W and a pressure of 2 mbar presented in Fig. 4(a) show that all samples from $c = 2.7\%$ to 100% (H_2 flow from 3000 to 0 sccm) correspond to the microstructure transition region with a crystallinity factor of around 50%. Moreover, reduction of the hydrogen flow rate increases the deposition rate by a factor up to 3.5 (Fig. 4(b)). This increase of the deposition rate with the silane concentration (at a constant silane flow rate) can be explained by the reduction of silane pumping loss due to the increase of the gas residence time by reducing the total flow rate. The deposition rate and the silane depletion as a function of silane initial concentration can be deduced (dashed lines in

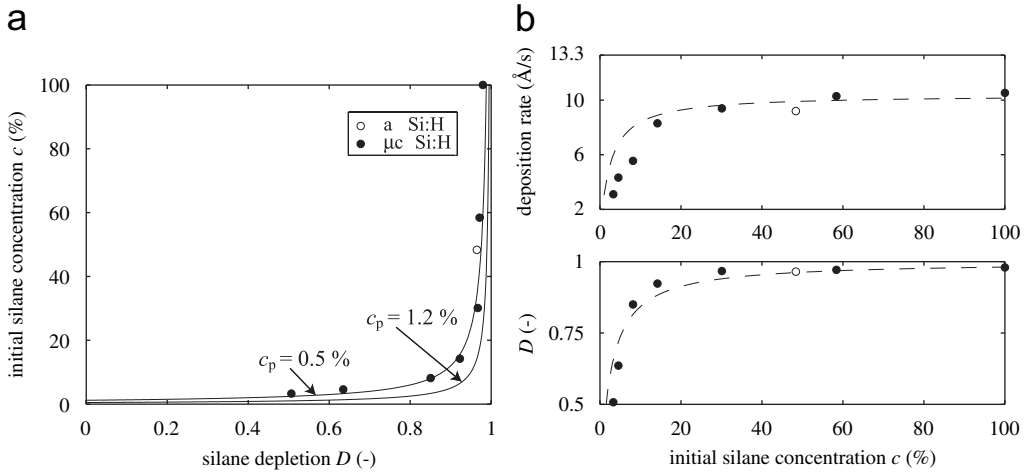

Fig. 4. (a) Plot of the transition zone and experimental data for µc-Si:H (•) and a-Si:H (○) samples as a function of the silane depletion and the silane concentration. (b) Measured (○, •) and modeled (- - -) deposition rate (top) and silane depletion (bottom) as a function of silane concentration from 2.7% to 100% in hydrogen. All samples were deposited with a silane flow rate of 82 sccm, a total pressure of 2 mbar and an input power of 1000 W.

Fig. 4(b)) from the silane dissociation efficiency η, (corresponding to the dissociated fraction of the silane flow) introduced in Refs. [6,11]:

$$\eta = \frac{D}{1 + (1 - D)c}, \tag{6}$$

and by using constant silane flow rate, pressure and dissociation frequency and assuming a probability that silane dissociation products contribute to film growth of 0.75 (see Section 3.4). The previous expression can be re-written using Eq. (3) as

$$\eta = \frac{1 - c_p/c}{1 + c_p}, \tag{7}$$

showing that the maximum silane dissociation efficiency is reached for pure silane ($c \to 1$) for a given material crystallinity (constant c_p [11]).

Moreover, experiments presented in Fig. 4(b) are in good agreement with the previous equations and show clearly that in terms of silane utilization efficiency, pure silane plasmas are the most efficient. Thus, microcrystalline silicon ($\phi_c = 60\%$) has been deposited from a pure silane plasma at a rate of 10.5 Å/s corresponding to the target deposition rate fixed previously.

3.3. Pure silane regime optimization

To optimize the pure silane regime, the only remaining adjustable process parameters are the RF input power and the working pressure. The effects of the RF input power on the deposition rate and on the silane depletion (and thus on the crystallinity) are presented in Fig. 5(a). We can distinguish two different regimes separated by a maximum in the deposition rate (12.3 Å/s) at a RF power input of 500 W. For lower power densities, since the silane flow rate is constant, the deposition is rate limited by the lack of availability of silane dissociation products for deposition, because the silane depletion fraction is low (down to 0.547 at 150 W in Fig. 5(a)) and the silane concentration in the plasma remains too high for µc-Si:H deposition for such low depletion. On the other hand, for higher power densities, when the silane depletion fraction approaches one, the deposition rate falls because part of the dissociation products are lost in the pumping line in the form of polysilanes or powder. The transition from a-Si:H to µc-Si:H deposition in Fig. 5(a) takes place between 500 and 750 W, corresponding to a relatively low power density of 0.19−0.28 W cm^{-2}. Moreover, the deposition rate at the transition from a-Si:H to µc-Si:H, 11.5 Å/s, is the closest to the maximum possible deposition rate (13.3 Å/s if all silane is dissociated and deposited uniformly).

Results of deposition performed at a RF power input of 1 and 2 kW for pressures from 0.5 to 4 mbar are presented in Fig. 5(b) and show a maximum in deposition rate for a pressure of 2 mbar. At higher pressures, for both power levels, deposition rates decrease slightly with pressure. We believe that this is mainly because of the higher powder formation caused by the increase of silane dissociation product density and not because of a pressure dependence of the power coupling since the silane depletion fraction is stable around one (bottom Fig. 5(b)). The strong decrease in deposition rate when the pressure is decreased from 2 to 1 mbar is also not attributable to a reduction of the silane depletion and has also been observed for H_2 diluted plasmas [14,27]; it could be induced by a non-uniform plasma in the reactor with a higher density plasma around the glass substrate at low pressure, hence consuming more silane without affecting in a significant manner the thickness uniformity over the substrate area. The downward shift in deposition rate over the whole pressure range between the two curves performed at 1 and 2 kW, can be plausibly attributed to the higher powder formation at higher power input [3] as seen in Fig. 5(a). Even if the step in deposition rate between 1 and 2 mbar is not well

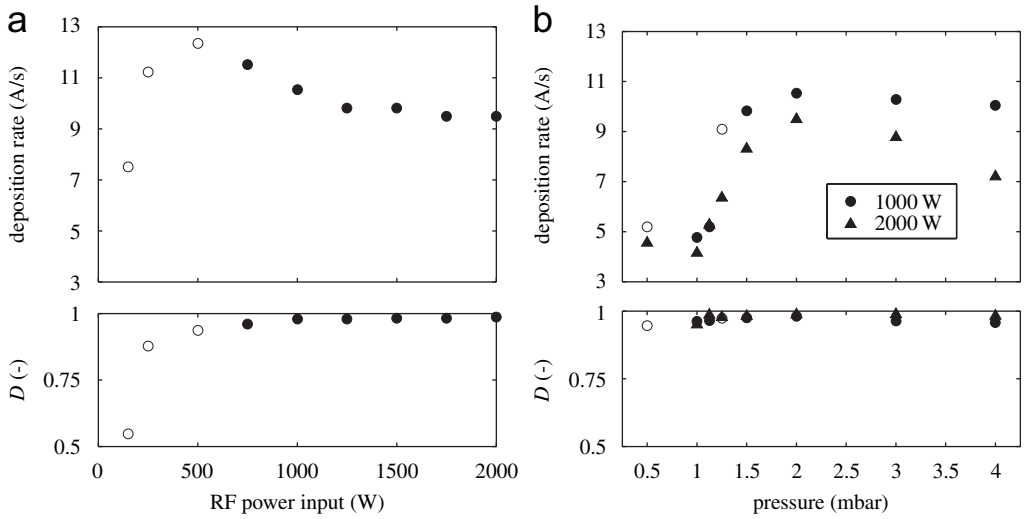

Fig. 5. Deposition rate (top) and silane depletion (bottom) as a function of (a) RF input power performed at a pressure of 2 mbar and (b) pressure performed with RF power input of 1 (•) and 2 (▲) kW from pure silane plasmas. Silane flow rates were 82 sccm. Open and full symbols correspond to a-Si:H and μc-Si:H, respectively.

understood, Fig. 5(b) confirms that the so-called "high-pressure depletion" regime [7,14,28] is interesting in terms of deposition rate and that—for the power inputs used—the pressure has no major effect on the crystallinity and all μc-Si:H samples have a crystallinity factor between 50% and 60% and even transition samples (○) contain a crystalline fraction of 46% and 36% for the samples at 0.5 and 1.25 mbar (see Fig. 5(b)), respectively.

3.4. Estimation of the polysilane or powder quantity

In Section 2, the silane flow rate was calculated in order to achieve a deposition rate of 10 Å/s. For the estimate of 82 sccm, it was assumed that (i) almost all the silane is consumed in the plasma, but that a fraction of up to 25% of the dissociation products is lost in the pumping line in the form of powder or polysilanes and (ii) the deposition rate (and thus the film thickness) is uniform over the whole electrode area including the substrate. In a totally polysilanes or powder pumping free process (i.e. all Si atoms contribute to film growth) with an input silane flow rate of 82 sccm, according to Eq. (5), the maximum achievable deposition rate is 13.3 Å/s. Deposition rates above 10 Å/s observed in Fig. 5(a) and (b) can be due either to processes producing a very small fraction of polysilanes (less than 25%) or to a non-uniform deposition rate distribution.

Deposition at 500 W (2 mbar, 82 sccm of silane) shows that the film thickness uniformity, presented in Fig. 6, is ±15% over the whole substrate area (including the non-uniformities due to the edge of the substrate and to the perturbation by the pumping side (see Fig. 6)). If only the central part ($27 \times 37\,cm^2$) of the substrate is considered (dashed rectangle in Fig. 6), the deposition rate non-uniformity falls to ±4%. Similar uniformities have been

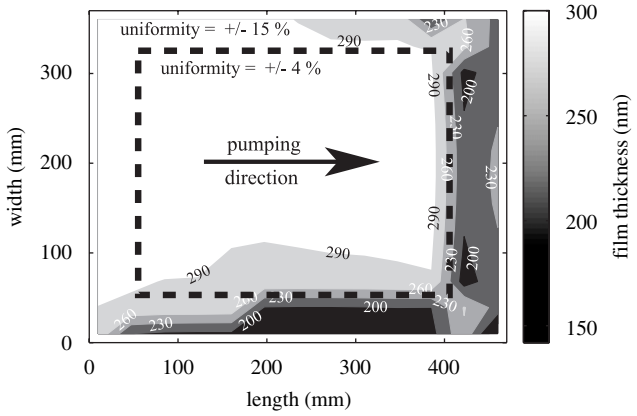

Fig. 6. Thickness uniformity measured by light interferometry for deposition performed at 500 W at a pressure of 2 mbar and a silane flow rate of 82 sccm.

found for depositions at different conditions (pressure, power, etc.) using pure silane. With regard to these observations, we can assume that the deposition rate is uniform over the whole substrate area in the range of around ±10% without taking into account the local effect of the substrate edge.

Because of this good uniformity, the deposition rate measurement can be used with the silane input flow rate and the depletion measurement to estimate the fraction of the input silane flow rate transformed into powder or polysilanes which are lost in the pumping line. In fact, the silane flowing into the reactor can be affected in three different ways: (i) a fraction of SiH_4 is not dissociated and is pumped out without having any reaction with reactor walls or other gas molecules, (ii) a fraction of SiH_4 is dissociated and is deposited and thus contributes to the deposition rate, or (iii) a fraction of SiH_4 is dissociated and

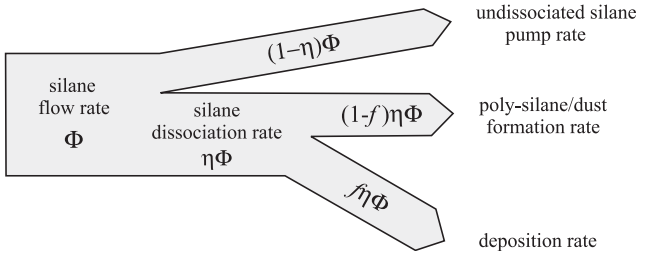

Fig. 7. Schematic representation of overall silane utilization. An input silane molecule can be either undissociated, dissociated and transformed into polysilanes or powder, or dissociated and contribute to film growth.

is pumped out in the form of polysilanes or dust particle. As summarized in Fig. 7, the fraction of undissociated silane flow rate corresponds to $(1-\eta)$, where η is the dissociation efficiency (Eq. (6)), the fraction of silane that contributes to film growth rate corresponds to $f\eta$, where f is the deposition rate efficiency, i.e. the probability that silane dissociation products contribute to film growth, and finally the fraction of silane transformed into polysilanes or powder which are lost in the pumping line corresponds to $(1-f)\cdot\eta$.

The fraction $f\eta$ of the silane flow that contributes to film growth rate is represented by the ratio $R/R_{\max}$ of the measured deposition rate to the maximum possible deposition rate (Eq. (5)). Using the definition of η in Eq. (6), we finally obtain an experimental estimation of the fraction of the silane input flow transformed into polysilanes or powder that is pumped away

$$(1-f)\eta = \frac{D}{1-(1-D)c} - \frac{R}{R_{\max}}. \tag{8}$$

According to the ±15% non-uniformity of the deposition rate mentioned previously, the maximum powder fraction for depositions performed at 500 W (a-Si-H, 12.3 Å/s, 2 mbar) and 750 W (μc-Si-H, 11.5 Å/s, 2 mbar) are 9% and 19%, respectively, which remains below the initial assumed threshold value (25%) of silane losses (Section 2). Note that this fraction does not give any information about the size of the polysilanes or powder particles.

4. Conclusions

The silane concentration in the plasma in a large area PECVD reactor has been determined using an in situ FTIR absorption measurement. Based on these measurements we have shown that the silane concentration in the plasma is a relevant factor to predict the microstructure of the deposited material and that it can be small enough even using pure silane in a RF discharge to allow microcrystalline silicon deposition as proven by ex situ Raman spectroscopy. To achieve such deposition without excessive RF input power, the silane flow rate has to be judiciously adjusted in order to have the lowest total flow rate as possible (the highest residence time), but with a sufficient silane flow rate to reach the target deposition rate. This approach fulfills the basic conditions of a suitable cost-effective process: a *uniform* layer (±15%) of microcrystalline silicon has been deposited over a *large substrate* ($37\times47\,\mathrm{cm}^2$) at *high rate* (11.5 Å/s) with an *efficient gas utilization* from a discharge producing a *low amount of powder* (19% of powder) with a *low power input* (750 W).

Acknowledgments

This work was funded by Swiss Federal Research Grant CTI 6947.1.

References

[1] J. Meier, R. Flückiger, H. Keppner, A. Shah, Appl. Phys. Lett. 65 (1994) 860.
[2] A. Shah, J. Meier, A. Buechel, U. Kroll, J. Steinhauser, F. Meillaud, H. Schade, D. Dominé, Thin Solid Films 502 (2006) 292.
[3] J.-L. Dorier, Ch. Hollenstein, A.A. Howling, U. Kroll, J. Vac. Sci. Technol. A 10 (4) (1992) 1048.
[4] W. Schwarzenbach, A.A. Howling, M. Fivaz, S. Brunner, Ch. Hollenstein, J. Vac. Sci. Technol. A 14 (1) (1996) 132.
[5] Y. Yin, M.M.M. Bilek, D.R. McKenzie, R.W. Boswell, C. Charles, Surf. Coatings Technol. 198 (2005) 379.
[6] A.A. Howling, L. Sansonnens, J. Ballutaud, F. Grangeon, T. Delachaux, Ch. Hollenstein, V. Daudrix, U. Kroll, in: 16th European Photovoltaic Solar Energy Conference, Glasgow UK, VB1, 2000, pp. 28–32.
[7] M.N. van den Donker, B. Rech, F. Finger, W.M.M. Kessels, M.C.M. van den Sanden, Appl. Phys. Lett. 87 (2005) 263503.
[8] T. Roschek, B. Rech, J. Müller, R. Schmitz, H. Wagner, Thin Solid Films 451–452 (2004) 466.
[9] L. Feitknecht, J. Meier, P. Torres, J. Zürcher, A. Shah, Sol. Energy Mat. Sol. Cells 74 (2002) 539.
[10] M. Sheib, B. Schröder, H. Oechsner, J. Non-Cryst. Solids 198–200 (1996) 895.
[11] B. Strahm, A.A. Howling, L. Sansonnens, Ch. Hollenstein, Plasma Sources Sci. Technol. 16 (2007) 80.
[12] B. Rech, T. Repmann, S. Wieder, M. Ruske, U. Stephan, Thin Solid Films 502 (1996) 300.
[13] J. Meier, U. Kroll, J. Spitznagel, S. Benagli, T. Roschek, G. Pfanner, C. Ellert, G. Androutsopoulos, A. Hügli, M. Nagel, C. Bucher, L. Feitknecht, G. Büchel, A. Büchel, in: Proceedings of 31st IEEE Photovoltaic Specialist Conference, Orlando, USA, 2005, p. 1464.
[14] U. Graf, J. Meier, U. Kroll, J. Bailat, C. Droz, E. Vallat-Sauvain, A. Shah, Thin Solid Films 427 (2003) 37.
[15] Y. Mai, S. Klein, R. Carius, J. Wolff, A. Lambertz, F. Finger, X. Geng, J. Appl. Phys. 97 (2005) 114913.
[16] A. Gordijn, J.K. Rath, R.E.I. Schropp, Prog. Photovoltaics 14 (2006) 305.
[17] J. Perrin, J. Schmitt, Ch. Hollenstein, A.A. Howling, L. Sansonnens, Plasma Phys. Controlled Fusion 42 (2000) B353.
[18] L. Sansonnens, A.A. Howling, Ch. Hollenstein, Plasma Sources Sci. Technol. 9 (2000) 205.
[19] L. Sansonnens, A.A. Howling, Ch. Hollenstein, Plasma Sources Sci. Technol. 7 (1998) 114.
[20] C. Droz, E. Vallat-Sauvain, J. Bailat, L. Feitknecht, J. Meier, A. Shah, Sol. Energy Mat. Sol. Cells 81 (2004) 61.
[21] A. Shah, J. Meier, E. Vallat-Sauvain, N. Wyrsch, U. Kroll, C. Droz, U. Graf, Sol. Energy Mat. Sol. Cells 78 (2003) 469.

[22] N. Pinto, M. Ficcadenti, L. Morresi, R. Murri, G. Ambrosone, U. Coscia, J. Appl. Phys. 96 (2004) 7306.
[23] M. Fukawa, S. Suzuki, L. Guo, M. Kondo, A. Matsuda, Sol. Energy Mat. Sol. Cells 66 (2001) 217.
[24] L. Qing-Song, W. Zhi-Meng, G. Xin-Hua, Z. Ying, X. Jian-Ping, Chin. Phys 14 (11) (2005) 2342.
[25] J. Ḱocka, T. Mates, H. Stućklıḱova, J. Stućhlık, A. Fekfar, Thin Solid Films 501 (2006) 107.
[26] Y. Tatsumi, H. Ohsaki, Density of c-Si, a-Si and a-Si:H, in: EMIS Data Reviews Series, vol. 1, Properties of Amorphous Silicon, INSPEC, London, 1989, p. 467–470.
[27] B. Rech, T. Roschek, J. ̈Muller, S. Wieder, H. Wagner, Sol. Energy Mat. Sol. Cells 66 (2001) 267.
[28] E. Katsia, E. Amanatides, D. Mataras, A. Soto, G.A. Voyiatzis, Sol. Energy Mat. Sol. Cells 87 (2005) 157.